Age-Related Changes in Visually Evoked Electrical Brain Activity

Gijs Plomp,[1]* Marina Kunchulia,[2] and Michael H. Herzog[1]

[1]*Laboratory of Psychophysics, Brain Mind Institute, School of Life Sciences, Ecole Polytechnique Fédéral de Lausanne, Lausanne, Switzerland*
[2]*Department of Behaviour and Cognitive Functions, I. Beritashvili Institute of Physiology, Tbilisi, Georgia*

◆ ━━━━━━━━━━━━━━━━━━━━━━━━━━━━━━━━━━━━ ◆

Abstract: Whereas much is known about the degenerative effects of aging on cortical tissue, less is known about how aging affects visually evoked electrical activity, and at what latencies. We compared visual processing in elderly and young controls using a visual masking paradigm, which is particularly sensitive to detect temporal processing deficits, while recording EEG. The results show that, on average, elderly have weaker visual evoked potentials than controls, and that elderly show a distinct scalp potential topography (microstate) at around 150 ms after stimulus onset. This microstate occurred irrespective of the visual stimulus presented. Electrical source imaging showed that the changes in the scalp potential resulted from decreased activity in lateral occipital cortex and increases in fronto-parietal areas. We saw, however, no evidence that increased fronto-parietal activity enhanced performance on the discrimination task, and no evidence that it compensated for decreased posterior activity. Our results show qualitatively different patterns of visual evoked potentials (VEPs) in the elderly, and demonstrate that increased fronto-parietal activity arises during visual processing in the elderly already between 150 and 200 ms after stimulus onset. The microstate associated with these changes is a potential diagnostic tool to detect age-related cortical changes. *Hum Brain Mapp 33:1124–1136, 2012.* © **2011 Wiley Periodicals, Inc.**

Key words: aging; backward masking; electroencephalography (EEG); temporal processing; visual perception

◆ ━━━━━━━━━━━━━━━━━━━━━━━━━━━━━━━━━━━━ ◆

INTRODUCTION

Aging has profound effects on cortex, such as shrinking [Resnick et al., 2003] and thinning [Salat et al., 2004], that come together with changes in cortical function such as, for example, the loss of functional specificity [Park et al., 2004] and decreased inhibitory control [Gazzaley et al., 2005, 2008]. Age-related changes in cortical functioning often manifest themselves as changes in functional brain networks [e.g. Grady et al., 2009], where typically occipital areas show decreased activity and frontal ones show increased activity [Davis et al., 2008; Grady et al., 1994], possibly acting as a compensatory mechanism [Gutchess et al., 2005; Park and Reuter-Lorenz, 2009]. Because these studies used hemodynamic measures, with excellent spatial but low temporal resolution, little is known about how aging affects the dynamics of brain activity and at what latencies after stimulus onset. Here we combined topographical analysis of averaged visual evoked potentials (VEPs) and electrical source imaging to investigate how aging affects visually evoked electrical activity in a visual discrimination task with masked vernier stimuli.

Vernier acuity is a good tool for studying cortical processing in elderly. Even though vernier stimuli and their
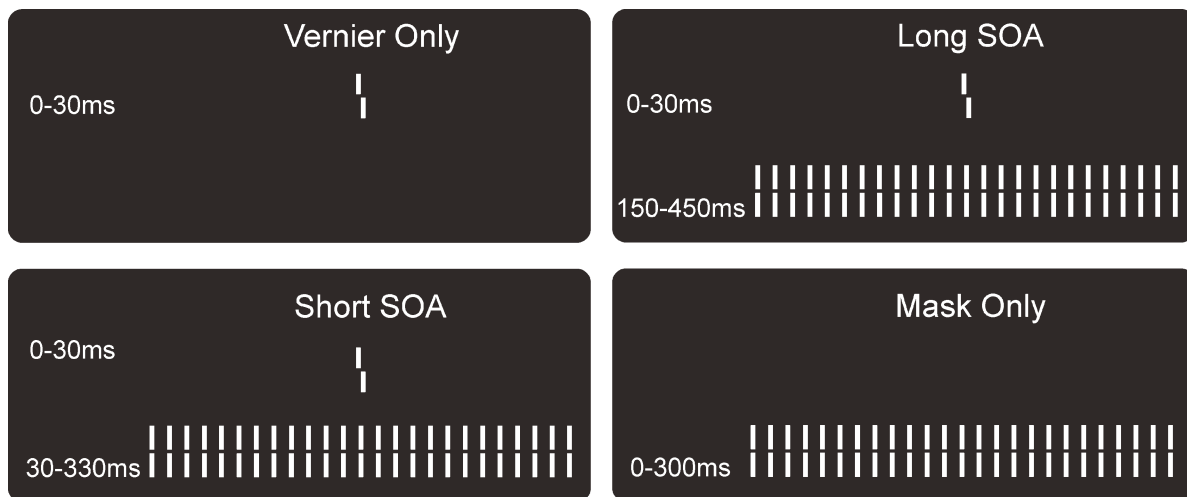
Figure 1.
The four stimulus conditions. The task was to discriminate the offset direction of a vernier stimulus that was presented for 30 ms in the center of the screen. The long and short SOA durations were chosen in order to yield similar performance levels for elderly and controls, respectively.

offsets are small, their VEPs can be reliably measured [Levi et al., 1983]. In a typical vernier discrimination task, two vertical bars are presented with a slight horizontal offset. Observers indicate whether the vernier is offset to the left or right. Young adults can typically discriminate offset sizes in the range of 10–20 arcsec, i.e. smaller than photoreceptor size. Discrimination of such small offset sizes can only be achieved by integration of information across, at least, a few photo-receptors [Westheimer, 1975]. For this reason, it is usually assumed that vernier acuity is mainly processed at cortical sites. In line with this, the VEP topographies suggest that verniers evoke widespread extrastriate activity [Srebro and Osetinsky, 1987]. Vernier discrimination is largely resistant to optical blur and therefore vernier thresholds do not vary much with age [Fahle and Daum, 1997; Garcia-Suarez et al., 2004; Lakshminarayanan and Enoch, 1995; Li et al., 2000]. Moreover, vernier acuity is also largely unaffected by retinal illuminance [Waugh et al., 1993; Li et al., 2000]. For this reason, vernier stimuli are a good tool for studying age-related cortical changes in visual processing.

In a recent study, we combined vernier acuity with a backward masking paradigm to study temporal visual deficits in aging (Roinishvili et al., in revision). A vertical vernier was followed by a masking grating comprised of 5 or 25 aligned verniers. If the grating has 25 elements, vernier offset discrimination is typically better than when it has five elements (the shine-through effect, Herzog and Koch, [2001]). The different masking effects of the two gratings cannot be explained by retinal mechanisms only. On a retinal level, the 25 element grating should deteriorate performance more strongly than a five element grating because the former has more elements and hence should mask stronger. But controls typically show good perform-

ance with a 25 element mask, while elderly show strongly deteriorated performance under these conditions (Roinishvili et al., in revision). We attributed this age-related effect to dysfunctions of visual and attentional processing in the elderly, particularly because several alternative explanations can be excluded. Among these are: optical deficits such as cataract (because vernier acuity is largely resistant to blur), memory and executive dysfunctions (because the task and the stimulus-response mapping are very simple and were well understood by the participants as evidenced by the good performance for unmasked vernier stimuli), and motor dysfunctions (because responses were not speeded). The strong masking effects in elderly are in line with the observation that processing slows down with age, affecting cognition and behavior [Birren and Fisher, 1995; Park and Reuter-Lorenz, 2009; Salthouse, 1996]. Evidence for slowed neural processing comes also from VEP studies. In particular, the first positive evoked component (P1) is delayed in elderly in general [Dustman et al., 1993], and also with vernier stimuli [Li et al., 2001]. Here we tested the hypothesis that the deficit for masked verniers stems from the slowing of cortical processes in elderly.

We recorded EEG for verniers with offsets that both young controls and elderly could discriminate well (see Fig. 1). If visual processing is slowed down in elderly, but qualitatively similar, then elderly should show the same progression of scalp topographies, or so-called microstates [Lehmann et al., 1987; Michel et al., 2001; Murray et al., 2008; Pascual-Marqui et al., 1995], but with longer durations. Microstates reflect the sum of electrical brain activity and provide a measure of the state of the brain. We used two masking conditions, one in which the mask immediately followed the vernier and one in which the SOA was 150 ms. Elderly behave poorly when the mask

TABLE I. Average statistics of the two observer groups

	Age (range)	Sex (m/f)	Acuity (s.d.)	Education (s.d.)
Elderly	66 (60–76)	10/9	1.10 (0.24)	16 (2.53)
Young controls	25 (19–32)	8/7	1.76 (0.23)	16 (2.46)

immediately follows the vernier (temporal processing deficit), but better when the mask comes later. The 150 ms SOA was chosen such that elderly had similar accuracy in this condition as the normal controls in the short SOA condition. In these performance-equated conditions, the VEPs of elderly and controls were hypothesized to be qualitatively similar, because presumably the vernier is in the same processing stage when the mask arrives, due to slow processing of elderly.

MATERIALS AND METHODS

Observers

The observers were 21 right-handed elderly with ages ranging between 60 and 76 years of age (mean 66, ± 4.6 s.d., 11 female), of which two EEG data sets were not analyzed due to excessive recording artifacts. As a control, 15 young observers with ages ranging between 19 and 32 years (mean 25, ± 4.2, 8 female) participated in the experiment. All observers had normal or corrected-to-normal vision with visual acuity of at least 0.8 in at least one eye [Bach, 1996]. The two groups had comparable years of education, see Table I. All observers were healthy and showed no signs of dementia and all understood the task without problems. Observers gave informed consent before the experiment. All procedures complied with the Declaration of Helsinki and were approved by the local ethics committee.

Stimuli and Apparatus

The stimuli consisted of white verniers and gratings presented on a black background, for 30 and 300 ms, respectively. A vernier consisted of two vertical line segments of 10′ (arc min) that were separated by a gap of 1′. The segments had a fixed horizontal offset of 71″ (arc sec) for every observer and condition. The grating consisted of 25 non-offset verniers, separated horizontally by 3.33′ and subtending 83′.

There were four stimulus conditions (see Fig. 1). In the Vernier Only condition, a single vernier was presented. In the Short SOA condition, the grating followed the vernier with a 30 ms SOA. In the Long SOA condition, the SOA was 150 ms. In the Mask Only condition, no vernier was presented but only the grating. The discrimination accuracy in the Mask Only condition was calculated by comparing the observer's response (left, right offset) to a dummy offset. This dummy offset was randomly chosen by the stimulus program to be left or right on each trial, but was not presented on screen (since no vernier was presented in the Mask Only condition).

The stimuli appeared on a Samsung SyncMaster 957DF CRT screen with a 100 Hz refresh rate. Maximal screen luminance was about 100 cd/m^2, as measured with a GretagMacbeth Eye-One Display 2 colorimeter. The background luminance on the screen was below 1 cd/m^2. Observers were seated in a dimly lit room at 3.5 m from the monitor. At this distance one pixel covers about 18″.

Procedure

Observers were instructed to report the perceived offset direction of the vernier and to guess when they were not sure. Accuracy was emphasized over speed. The stimulus conditions were not fully explained until after the experiment.

The vernier offset direction was chosen randomly for each trial, except in the Mask Only condition, where no vernier was presented (and a dummy offset was chosen in order to compute an accuracy score). The inter trial pause varied randomly between 1,000 and 1,500 ms. The four stimulus conditions were randomly interleaved and presented in recording runs of 80 trials, in which each condition appeared 20 times. The experiment consisted of 8 runs so that 160 repetitions of each stimulus condition were presented to each observer.

EEG Recording and Data Processing

The EEG was recorded with a BioSemi Active Two system (BioSemi, Amsterdam, the Netherlands) using 64 Ag-AgCl sintered active electrodes positioned in a cap according to the 10–20 system. The recording was referenced to the CMS-DRL ground, a feedback loop that keeps the montage potential close to amplifier zero. The electrodes creating the loop are positioned left and right to POz. We recorded the electro-oculogram (EOG) with electrodes 1 cm above and below the right eye, and 1 cm lateral to the left and right outer canthus. The recording sampling rate was 2048 Hz. Off-line, the data were downsampled to 512 Hz and notch filters were applied to remove 50 Hz and monitor noise. The data were band-pass filtered between 0.1 and 40 Hz using a Butterworth filter with −12 db/octave roll-off. We visually inspected all data to determine noisy electrodes.

We selected epochs between −100 and 400 ms around stimulus onset and did semi-automatic artifact detection with a threshold of 75 μV for the EEG and EOG electrodes. We excluded noisy electrodes, as determined by visual inspection of the individual recordings, from the artifact-rejection procedure. These electrodes were later interpolated. For the elderly, on average 4.5% of epochs were rejected, for the controls 6.7% of epochs was rejected.

We removed DC drift by subtracting the average across the epoch and then averaged the selected epochs within

observer and stimulus condition. The averaged epochs were re-referenced to the average reference. No correction for prestimulus amplitudes was applied. We interpolated the noisy electrodes using 3D spline interpolation [Perrin et al., 1987]. The number of interpolated electrodes was on average 0.5 for elderly, and 0.7 for controls. Across observers, grand averages per condition were computed after normalizing the individual averages to their global field power (GFP) across the entire epoch, to assure even contributions of individual averages to the grand average amplitudes. The GFP is the standard deviation of the electrical potentials across the electrodes and is a measure of the response strength [Lehmann and Skrandies, 1980].

Topographic Segmentation Analysis

The topographic analysis examined the spatial variations of the scalp potential topography over time, between conditions and groups [Blanke et al., 2005; Michel et al., 2001, 2004; Murray et al., 2005]. We segmented the continuous grand average VEPs into a succession of discrete template maps using the Atomize and Agglomerate Hierarchical Clustering (AAHC) algorithm [Murray et al., 2008], a spatio-temporal clustering algorithm [Lehmann et al., 1987; Pascual-Marqui et al., 1995]. This characterizes each epoch as a succession of a limited number of template maps without prior assumptions about the temporal characteristics of the data. The result reflects how scalp potential maps remain in a quasi stable configuration for certain periods, and then change to a new spatial configuration.

The number of template maps that best explains the data across conditions was determined by the absolute minimum in the Cross Validation (CV) value [Pascual-Marqui et al., 1995]. The CV value is a ratio of the global explained variance of the AAHC result and the degrees of freedom in the model (the number of maps). Therefore, the number of template maps is determined in a data-driven way, optimizing the fit to the epochs while keeping the number of maps as low as possible. Two template maps were merged into one when their spatial correlation exceeded 90%, and maps smaller than 6 time points (12 ms) were merged with the neighboring map that correlated highest with the small segment. The analysis accounted for voltage polarity so that potential maps with similar topography, but inverted voltages were treated as different maps.

The segmentation results were inspected for commonalities across conditions and groups, and for differences between them. Differences in template maps (also: microstates) point to differences in the underlying brain activity because whenever the spatial configuration of the electric field on the scalp changes, the underlying electrical sources must have changed as well [Michel et al., 2004].

To determine the duration with which template maps were present for each observer, we compared the template maps to the instantaneous scalp potential maps in individual VEPs using a competitive fitting procedure. For each time point of the individual epochs, the scalp topography was compared to each template map present in the grand-average at that time by means of normalized spatial correlation. The time point was then labeled according to the template map that correlated best. From this fitting procedure we determined the duration that a given map was observed in each condition, across a given time period (frequency of occurrence). The time period (114–173 ms) was determined on the basis of the first onset and last off-set of the map of interest in the grand average topographical analysis. To assess the statistical reliability of the differences in average observed frequencies of occurrences between groups (Elderly - Control) we used nonparametric bootstrapping ($n = 5,000$) of the difference scores. A nonparametric approach was necessary because the observed frequencies were not normally distributed (due to the presence of 0 values for control subjects). We calculated the 95% confidence interval of the bootstrapped differences for each stimulus condition using the adjusted bootstrap percentile (BCa) method. This way we determined whether the group difference could be reliably distinguished from zero.

GFP Analysis

We compared the GFP of the average individual VEPs between groups (Elderly, Controls) in each of the four stimulus conditions with unpaired t-tests and a significance threshold of $P < 0.05$. GFP was compared between 0 and 400 ms, at 205 consecutive time-points.

Source Analyses

We estimated current densities from the average data for each condition and observer using a Local Auto-Regressive Average (LAURA) inverse solution [Grave de Peralta Menendez et al., 2001, 2004; Grave de Peralta Menendez and Gonzalez Andino, 2002; Michel et al., 2004]. To create an inverse solution, we defined a solution space of 4,022 evenly spread source points within the gray matter of the Montreal Neurological Institute's (MNI) 152 template brain. We transformed the MNI volume to a best fitting sphere (SMAC model; Spinelli et al., 2000) and used a 3-shell spherical head model to calculate the lead field for the 64 electrodes and the LAURA inverse solution. This way, we estimated current densities (CD, mA/mm^3) throughout the source space for each observer at each time point for each condition.

The localization accuracy of LAURA has previously been demonstrated in epilepsy studies with electrical source imaging alone [Brodbeck et al., 2009] and in combined EEG-fMRI studies [Groening et al., 2009; Vulliemoz et al., 2009]. In addition, LAURA has been successfully used to determine neural aspects of e.g. embodiment [Arzy et al., 2006; Blanke et al., 2005], auditory perception

[De Santis et al., 2007; Spierer et al., 2007], visual perception [Plomp et al., 2009, 2010], and multisensory interactions [Murray et al., 2005]. Although a denser sampling on the scalp (more electrodes) can increase the accuracy of source localization, the relation is not a linear one and accuracy flattens off at around 100 electrodes [Michel et al., 2004]. This means that good results can still be obtained using sparser setups (see for example Gonzalez Andino et al., [2007]).

We statistically analyzed CD amplitudes in two separate analyses. The first analysis consisted of a two-way repeated measures ANOVA [Pinheiro and Bates, 2000] with the factors Condition and Group, and had observers as a random factor. This analysis was to investigate Group effects while taking into account the variability induced by the stimulus conditions. The analysis was restricted to those latencies where group differences were observed across stimulus conditions in the topographical or the GFP analysis. In total, 201,100 (4,022 source points × 50 time points) ANOVAs were calculated. The second analysis focused on the Short SOA condition and assessed Group differences using unpaired t-test. This analysis was done time-point wise throughout the entire epoch (−100 to 400 ms), in 1,029,632 tests (4,022 source points × 256 time points). In both analyses CDs were normalized within observers by the average GFP across conditions. The primary reason for such normalization is to reduce intersubject variance and enhance the sensitivity of the test. The normalization allows for the analysis of relative differences in source strength between groups or conditions. We controlled for multiple testing by setting the False Discovery Rate [FDR; Benjamini and Hochberg, 1995; Genovese et al., 2002] to 0.05 for each effect, at every time point. Where the results did not survive FDR correction, we set the threshold for statistical significance such that it highlighted the regions of maximal difference between conditions. This was the case for the Group effect of the ANOVA results, where the threshold was set to 0.0005. The ANOVAs and FDR thresholds were calculated using R [R-Development-Core-Team, 2008]. The EEG data processing and analyses were performed using the Cartool software (http://brainmapping.unige.ch/Cartool.htm).

RESULTS

Accuracy

The largest deficit in discrimination accuracy for elderly occurred with short SOAs. In that condition elderly scored 59% correct as compared to 83% for the controls. Elderly were also less accurate than controls in the Vernier Only (87% correct vs. 96%) and Long SOA (84% vs. 95%) condition. The accuracy of elderly in the Long SOA condition (84%) was comparable to that of controls in the Short SOA condition (83%). Figure 2 depicts the mean accuracy and 95% confidence for elderly and controls in the four stimulus conditions.
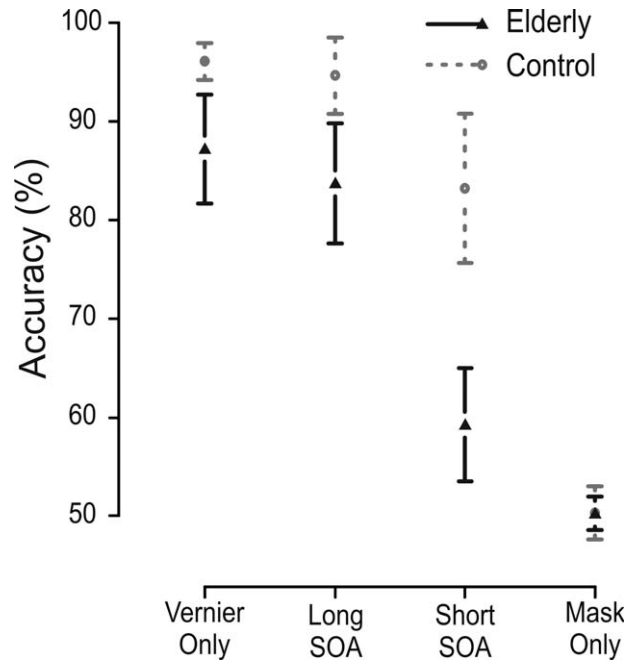

Figure 2.

Behavioral results. Elderly showed particularly large deficits when the mask immediately followed the vernier (Short SOA condition, 30 ms SOA). Performance for elderly in the long SOA condition resembles that of controls in the short SOA condition, as aimed for. Because vernier durations were short, vernier discrimination was slightly affected in the elderly (Vernier Only condition). In the Mask Only condition, no vernier was presented and performance is about chance level (50%). Error bars denote 95% confidence intervals.

Aging Effects in VEPs Across Stimulus Conditions

The segmentation analysis identified a template map (microstate) at around 150 ms that only occurred in elderly, for all stimulus conditions (template map 3, Fig. 3). The microstate is characterized by a central positivity and occurred between 114 and 173 ms across conditions. The frequencies of occurrence for this microstate in elderly and controls are listed in Table II. Bootstrapping analysis showed that the Group differences in frequency of occurrence could be reliably distinguished from zero. The 95% confidence intervals showed no overlap with zero (CI for Vernier Only: 2.1–11.7 time points; Long SOA: 4.6–13.0; Short SOA: 5.0–12.8; Mask Only: 3.7–11.0). Therefore this microstate occurs more often in elderly than controls, irrespective of the stimulus condition.

This microstate (template map 3) also occurred in controls, but at latencies after 350 ms. Its occurrence in controls was restricted to the Mask Only condition. For elderly too, the map recurred at longer latencies, but the recurrence was restricted to the Mask Only and the Short SOA condition (the two most difficult conditions).
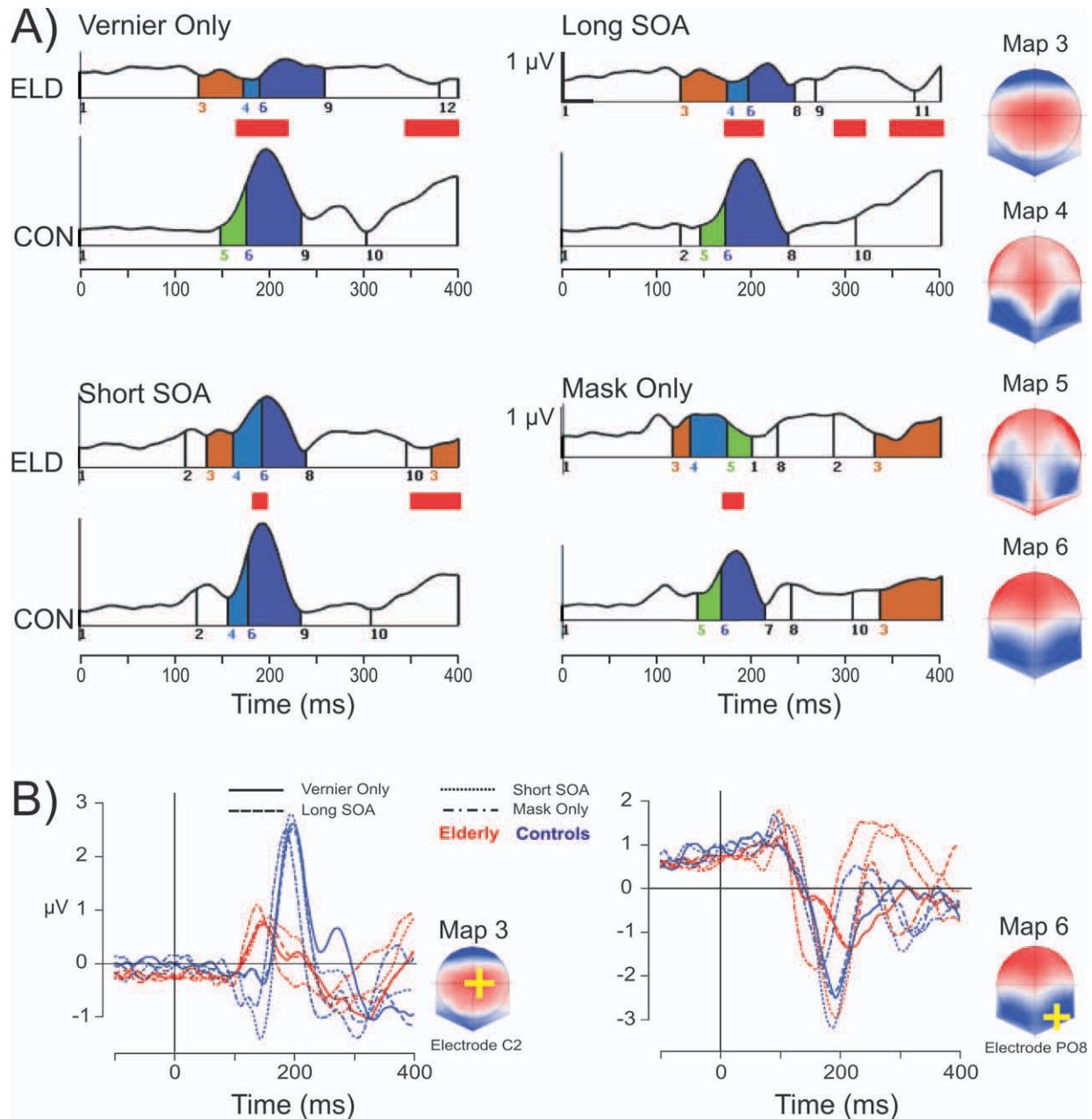
Figure 3.

Results of the scalp EEG analysis. Panel **A** shows the topographical segmentation results for elderly (ELD) and young controls (CON) in each stimulus condition, with the GFP on the ordinate and time on the abscissa. The vertical lines indicate microstate onset and offset. Microstates have consistent colors and numbers across the eight subplots. The integer numbers on the abscissa correspond to the voltage topographies on the right (average reference, nose on top). Latencies of significant GFP differences between elderly and young controls are indicated by red bars. Smaller GFP for the elderly was seen at around 200 ms after stimulus onset during the occurrence of template map 6, for all conditions. At around 150 ms, template map 3 selectively occurred for the elderly, for all conditions. The C2 location is the location of maximum amplitude in map 3. Panel **B** depicts the grand average traces at the C2 electrode across stimulus conditions for elderly and young controls. Similarly, traces for the electrode with minimal amplitude in map 6 are depicted, reflecting the N1 component across conditions. [Color figure can be viewed in the online issue, which is available at wileyonlinelibrary.com.]

TABLE II. Average (s.d.) frequencies of occurrence in time points for map 3

Condition	Elderly	Control
Vernier only	8.2 (9.8)	1.9 (4.1)
Long SOA	10.5 (9.2)	1.9 (2.9)
Short SOA	9.5 (8.6)	0.9 (9.5)
Mask Only	7.5 (8.0)	0.6 (1.8)

We tested whether the frequency of occurrence of map 3 in the 114–173 ms range predicted the behavioral accuracy in the elderly. This was not the case across the three stimulus conditions containing a target vernier ($R^2 = 0.01$) nor within conditions (Vernier Only, $R^2 = -0.07$; Short Soa, $R^2 = 0.04$; Long Soa, $R^2 = -0.01$).

The GFP for elderly was significantly decreased in all stimulus conditions at around 200 ms (see Fig. 3). At this latency, the segmentation analysis showed a map with occipital negativity, which reflects the N1 component (template map 6, Fig. 3).

The VEP of elderly in the Long SOA condition does not resemble that of controls in the Short SOA condition, even though accuracy was similar for the two groups. The occurrence of template map 3 and the GFP decrease for elderly suggests that elderly attain the same performance level not because of slowed neural processing, but rather that elderly use qualitatively different neural processes.

We did electrical source imaging at the latency between the first onset of template map 3 and the last observed GFP difference around the N1 (115–212 ms). Significant Group effects were observed in nine different brain areas ($P < 0.0005$, uncorrected), the locations and latencies of which are detailed in Table III. Elderly showed smaller CDs in the precuneus and posterior cingulate, as well as in an extensive right-lateralized occipito-temporal region that included the occipital gyrus, the inferior temporal gyrus, and the fusiform gyrus. Elderly showed larger CDs in parietal (BA40) and frontal regions (including BA8, 9 and 10), as well as in the head of the caudate nucleus.

Figure 4 illustrates the locations of the three regions (out of six) that showed the longest effects (the precuneus, inferotemporal gyrus, and caudate nucleus), as well as the CD time series per condition in these regions.

In the left inferior frontal gyrus, and simultaneously with the Group main effect, a two-way interaction between Group and Condition was observed. This interaction indicates that elderly showed larger CDs than controls in all conditions (Vernier Only: elderly 1.4 vs. controls 1.1 mA/mm^3; Long SOA: 1.9 vs. 1.3; Short SOA: 1.5 vs. 1.3) except in the Mask Only condition (1.3 vs. 1.4 mA/mm^3; values from the center-of-mass source point). This suggests that for elderly the evoked activity in the left inferior frontal gyrus may be related to the target presence. In all other areas the Group effect was of the same sign across the four stimulus conditions and no simultaneous interaction effects were observed.

We tested whether the pattern of posterior decreases and fronto-parietal increases reflects a compensatory mechanism. In the case of compensation, the amount of occipital activity correlates negatively with the amount of frontal activity, and the increased frontal activity predicts better performance [Gutchess et al., 2005]. For areas that showed decreased activity for elderly (the precuneus/cingulate, and the right lateral occipital region), we correlated the average CD amplitude in the 115 - 220 ms latency with that of the frontal areas that showed increased activity in the elderly (Table III). No negative correlations were observed. Similarly, we correlated activity in frontal areas with behavioral performance but no positive correlations were observed. Rather, we obtained two significant negative correlations between accuracy and CDs, one in the right inferior parietal lobe (Pearson's product-moment correlation, $T(-3.55)$, $P < 0.001$) and one in the right inferior frontal gyrus ($T(-2.15)$, $P < 0.05$). These negative correlations were not observed for young controls. Taken together this means that decreased occipital activity did not predict increased frontal activity in our data, at these latencies, and that activity in frontal areas may hinder performance in the elderly.

TABLE III. Locations and latencies of significant group effects

Label (Brodmann Area)	Laterality	x, y, z*	Latencies (ms)	Effect
Precuneus (BA31)/Cingulate	Left	−9, −58, 23	130–140, 150–160	C>E
Medial and superior frontal gyrus (BA10)	Left	−9, 63, 3	160–164	E>C
Inferior parietal lobule (BA40)	Right	58, −33, 23	164–177	E>C
Inferior temporal, occipital, fusiform gyrus	Right	42, −50, 8	170–211	C>E
Caudate nucleus	Left	−14, 0, 20	171–191	E>C
Middle frontal gyrus (BA8/9)	Right	21, 37, 37	175–177	E>C
Precentral gyrus	Left	−44, 8, 9	179–183	E>C
Middle/inferior frontal gyrus	Right	52, 21, 29	179–191	E>C
Inferior frontal gyrus (BA9)	Left	−55, 4, 23	179–189	E>C**

*Talairach coordinates of the center of the area showing a significant Group effect ($P < 0.0005$, uncorrected).
**A simultaneous interaction between Group and Condition revealed that the Mask Only condition showed no difference between the groups in this area.
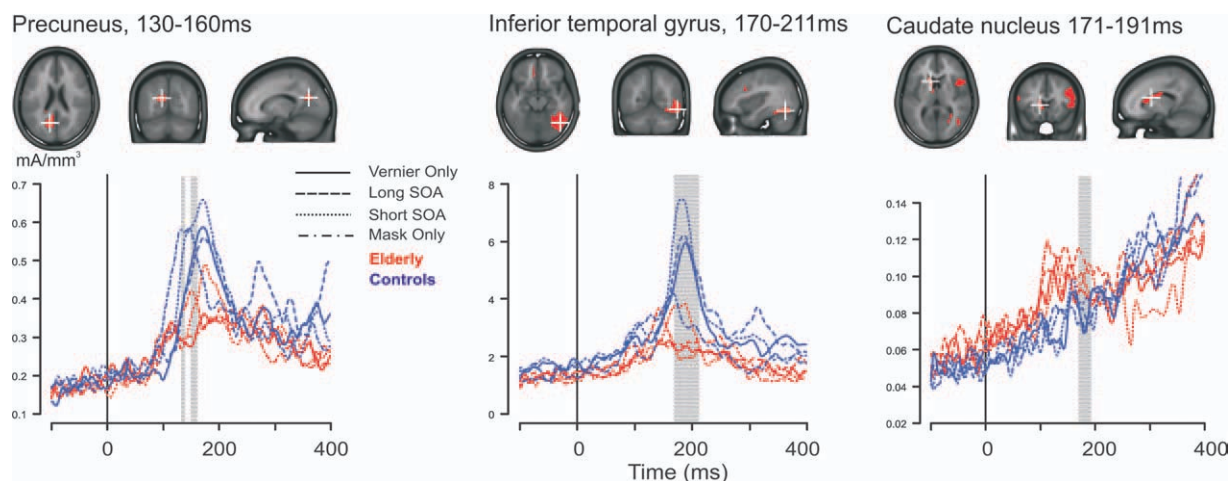
Figure 4.

The three brain regions with the longest lasting differences between elderly and young controls. Six additional regions showed a group effect (more details on all nine regions can be found in Table III). Each of the three upper panels shows in red the areas with statistically significant Group differences ($P <$ 0.0005, uncorrected), projected onto the MNI standard brain. To illustrate the group effect, current density (CD) time series are plotted for elderly (red) and controls (blue), for each stimulus condition. The time series come from the source point at the center of mass of the area that showed the Group effect. Latencies of significant differences are indicated by gray vertical bars. The black vertical bars indicate stimulus onset. Occipital areas showed decreased CDs for elderly, whereas frontal and medial ones showed increased CDs for elderly (see also Table III). [Color figure can be viewed in the online issue, which is available at wileyonlinelibrary.com.]

Aging Effects in VEPs, Short SOA Condition

Elderly had great difficulties discriminating the vernier offset direction when it was quickly followed by a mask, as expected. We separately analyzed the Short SOA condition to characterize the largest differences between elderly and controls throughout the epoch (−100 to 400 ms). Significant differences (corrected for multiple testing using a FDR of 0.05) appeared in three areas (see Fig. 5). The first area centered on the left lingual gyrus (−15, −58, 2) and included parts of the cuneus. Here, elderly showed decreased CDs around stimulus onset. Around the same latency a second area was found in the right fusiform gyrus (42, −49, −13). Both of these areas showed decreases for elderly around stimulus onset, but at between 150 and 160 ms after stimulus onset (see Table III, Group effect). The third area was in the left supramarginal gyrus (−59, −45, 23). Here elderly showed increased CDs at around 177 ms. The CDs in this area did not correlate with behavioral accuracy.

DISCUSSION

To study age-related differences in visually evoked brain activity, we used vernier stimuli in a visual masking paradigm while we measured the EEG. There are three main findings in our study. First, elderly show a microstate (VEP topography) that appears irrespective of stimulus condition at around 150 ms, and which is not present in young controls. Secondly, source analysis around this latency shows increased parietal and frontal activity in elderly, whereas occipito-temporal activity is decreased. Thirdly, we find that decreases in occipital activity already occur around stimulus onset.

Vernier discrimination is largely resistant to optical blur and is also largely unaffected by retinal illuminance [Li et al., 2000; Waugh et al., 1993]. Vernier discrimination typically declines only slightly with age [e.g. Lakshminarayanan and Enoch, 1995], making vernier stimuli a good tool for studying age-related visual processing. In our data, elderly show lower accuracy in the vernier only condition, in accordance with previous work [Roinishvili et al., in revision]. We attribute this slight deficit to the short presentation times (30 ms) used in our study.

Elderly and controls were carefully matched except for visual acuity which is, as always, deteriorated in the elderly. Deteriorated visual acuity, however, cannot account for the deteriorated masking as a single factor, as we showed previously using multiple linear regression analysis [Roinishvili et al., in revision]. It seems there are genuine temporal processing deficits in the elderly. In line with this, elderly have similar vernier offset discrimination performance as controls when the SOA is prolonged [Roinishvili et al., in revision], a finding that our current study replicates. For elderly, furthermore, discrimination performance strongly deteriorates when the mask immediately follows the vernier, while controls have little difficulty under this condition. It seems unlikely that low visual acuity only affects the Short SOA condition.

We hypothesized that elderly process visual stimuli more slowly and that this slowing results in discrimination deficits when the target is quickly followed by a mask. If this were the case, the microstates observed in the VEPs of elderly should have lasted longer, perhaps long enough so that in the two performance-equated conditions the VEP was qualitatively similar to that of controls. Contrary to our expectations, however, the VEPs show no effects of slowing, but instead show qualitatively different microstates, and decreased response strengths in the VEPs of elderly.

Elderly show a marked decrease in response strength around the N1 latency, in line with previous VEP aging effects for vernier stimuli [Li et al., 2001]. More interestingly, elderly display a scalp topography at around 150 ms that is qualitatively different from that of young controls (map 3, Fig. 2). This microstate is characterized by a positivity over central areas. Previous research has identified a similar microstate in the spontaneous EEG that is observed more frequently in old age [Koenig et al., 2002]. The apparent resemblance between this and our finding, however, is difficult to interpret because Koenig et al. analyzed spontaneous EEG activity, whereas our results concern averaged VEPs. Despite this, the convergence suggests it may be possible to use this microstate as a simple electrophysiological indicator of age-related changes in cortical function. To further validate this microstate as a diagnostic tool, longitudinal studies are needed that reveal how visual processing changes with increasing age, and how this is related to structural and functional changes as observed in (f)MRIs of the same subjects.

The distinct microstate for the elderly at around 150 ms may reflect changes in attentional processing. The microstate is also observed at latencies after 350 ms, in both elderly and controls, but only in the behaviorally difficult conditions, i.e. when the mask immediately follows the vernier or when no vernier is presented at all (see Fig. 3). In the latter condition (Mask Only), the microstate occurs in both elderly and controls. Since no target can be detected in this condition, the map may reflect a relatively late reorientation mechanism. This interpretation is consistent with our finding that elderly show increased activity across stimulus conditions in right inferior parietal areas that are involved in the reorienting of attention [Corbetta et al., 2000, 2008]. Previously, increased activity in inferior parietal areas (BA40) for elderly has been observed in PET and fMRI studies, and this activity may reflect increased spatial attention in the elderly that acts as a compensation mechanism for decreased input from sensory cortex [Grady et al., 1994; Gutchess et al., 2005]. From our data, however, it rather seems that activity increases in the right inferior parietal cortex (as in the right inferior frontal gyrus) hinder the task, while other fronto-parietal areas show no significant correlation with behavior. Furthermore, in the detailed analysis of the Short SOA condition increased left inferior parietal activity for elderly (see Fig. 5) did not correlate with subsequent behavior.

At around the latency of the parietal activity increase, additional increases were seen across conditions in the medial frontal gyrus, the superior frontal gyrus, and the caudate nucleus, while decreases were seen in the precuneus and the cingulate cortex (Table III). This pattern of increases and decreases occurs from around 160 ms after stimulus onset, at latencies of ongoing visual processing. The pattern demonstrates greater involvement of frontal and parietal regions for elderly in visual processing that seems to include the caudate nucleus. An increased role for the caudate nucleus in visual processing for elderly has previously been shown during visual target detection [Madden et al., 2004] and for memorizing visual scenes [Gutchess et al., 2005]. The most extensive activity decreases, in time and volume, were seen in higher-level visual areas of the occipito-temporal cortex between 170 and 210 ms. From the detailed analysis of the Short SOA condition (see Fig. 5), similar decreases were already evident around stimulus onset in right occipito-temporal areas, as well as in left occipital regions. This indicates that both ongoing and evoked activity in occipital areas are decreased in the elderly.

The posterior-anterior shift model of aging [Davis et al., 2008; Grady et al., 1994] posits that the degeneration of sensory areas in occipital cortex is compensated for by increased activity in frontal cortex [see also Park and Reuter-Lorenz, 2009]. Our data confirm that activity increases in frontal areas co-occur with activity decreases in occipital cortex in visual processing, but the increased frontal activity did not, however, predict increased task performance, neither in frontal nor parietal areas, nor in the caudate nucleus. The same held for the duration of the elderly microstate. In addition, the frontal activity increases did not correlate with decreases in posterior areas. Taken together, this strongly suggests that age-related changes in evoked electrical activity do not provide a clear benefit to the elderly, at least not at the early latencies we tested.

Other studies have also reported results that are difficult to reconcile with the frontal compensation theory. Although decreased VEPs for the elderly are often reported [Dustman et al., 1993; Li et al., 2001], increases have also been observed [Aine et al., 2006]. In auditory evoked responses too, eldery may show increased responses in both EEG [Pfefferbaum et al. 1980] and MEG signals [Aine et al., 2005; Pekkonen et al., 1995]. Elderly also show increased MEG responses to median nerve stimulation in primary somatosensory areas. This shows that elderly do not always have decreased activity in sensory areas limiting the scope of the compensatory hypothesis. In addition, elderly do not always show increased frontal activity. For example, Madden et al. [2004] reported similar prefrontal activity in elderly and controls in a visual detection task. In a memory task, decreased frontal activity has been observed at the encoding stage [Logan et al., 2002]. This under-recruitment could be remedied with the proper task instructions, so that frontal increases may be strongly task-dependent. Furthermore, it has been shown
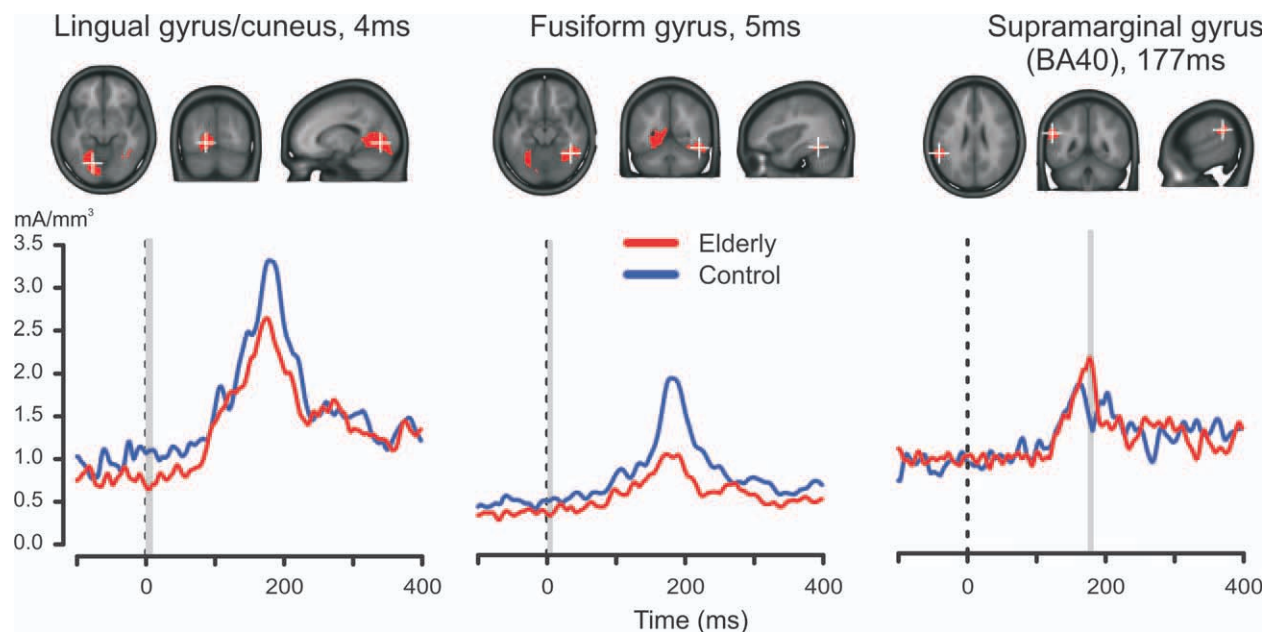
Figure 5.

Aging effects in the Short SOA condition. Each of the three upper panels shows in red the areas with statistically significant differences (FDR = 0.05 corrected). Peri-stimulus decreases were observed in the left lingual gyrus and parts of the cuneus (left panel), and in the right fusiform gyrus (middle panel). A stimulus-evoked increase for elderly was observed in the left in-ferior parietal cortex (right panel). The lower three plots show the corresponding current density timeseries at the regional source-point with minimal P-value. The black line indicates stimulus onset, the gray bars mark latencies of significant differences. [Color figure can be viewed in the online issue, which is available at wileyonlinelibrary.com.]

that frontal increases can be paradoxical. Calautti et al. [2001] show increased frontal activity for elderly that actually resulted from decreased frontal activity that was already present at rest. That is, controls had higher baseline activity in frontal areas before the stimulus, whereas elderly had to specifically recruit them. Our data also show distinct baseline activity for elderly (see Fig. 5). Such changes in activity may reflect changes in cognitive strategies, but can also result from structural changes in the elderly. Taken together, it seems that the pattern of decreases in sensory areas together with increases in frontal areas is not a universal one, and that when increases in frontal areas do occur, these do not automatically reflect compensatory mechanisms.

Age-related structural changes make it difficult to interpret observed activity changes [D'Esposito et al., 1999, 2003; Poldrack, 2000] between age groups. For example, age-related changes in neurovascular coupling complicate the interpretation of hemodynamic measures (PET, fMRI). Although EEG provides a more direct measure of neural activity, electrical activity is likely to change as a function of age-related brain plasticity. This is why we tried to relate changes in the observed activity to performance on the task. The fact that no such relations were found is in line with the idea that structural changes caused the observed patterns of activity in the elderly.

It could be that the effects we observe are due to life-span neural plasticity [Aine et al. 2006]. Changes in the (relative) white- and gray matter volumes in posterior and frontal areas, as well as changes in the connectivity between those areas could make them function differently with increased age. In this maturation account, the increased frontal activity is not compensating for decreased posterior activity, but co-occurs with it. This includes the possibility that the changed neural activity in the elderly supports their current behavioral performance. That is to say that their performance would be worse without (some of) these changes, but that local changes do not predict interindividual differences in performance. This is in line with our findings.

Besides compensation and maturation, the changed neural activity in elderly may also reflect neural deterioration. Elderly show decreased inhibitory control on several scales. Loss of inhibitory mechanisms leads to deteriorated surround suppression mechanisms in elderly, which in turn can lead to a paradoxical improvement in motion discrimination [Betts et al., 2005]. On a larger scale, elderly show impaired suppression of irrelevant distracters. In an fMRI study, elderly showed little suppression of activity for task-irrelevant stimuli in visual areas, but the greater this suppression, the better was their performance on a subsequent memory task [Gazzaley et al., 2005]. Using EEG measurements in the same paradigm, it was shown

that this suppression deficit manifests in P1 amplitudes and in N1 latencies [Gazzaley et al., 2005]. Whereas young controls show decreased P1 amplitudes and delayed N1 latencies for task-irrelevant stimuli, this is not the case for elderly. This suggests that top-down suppression of irrelevant visual processes is diminished in the elderly, which may result from deterioration in specific cortical areas. The dysfunctional activity we found in parietal areas may be an example of this, possibly resulting from decreased inhibitory processes.

Most of the increased activity in our data appears in cortical areas that are known to deteriorate in old age. The medial and inferior frontal gyrus and inferior parietal region (B40), among others, show decreased metabolism with age, as shown in a PET study [Pardo et al., 2007]. Furthermore, volume reduction of gray and white matter is most severe in parietal and frontal cortex [Resnick et al., 2003]. The cortical surface becomes thinner with age, and this process affects the regions for which we found increased activity in visual processing: the precentral gyrus and inferior frontal gyrus [Salat et al., 2004]. Although a possible compensation mechanism, increased activity in the elderly may therefore also indicate local dysfunction [Dickerson et al., 2004]. It seems therefore likely that the extra activity we observed in visual processing reflects age-related neural deterioration.

In conclusion, our results show that elderly have qualitatively very different VEP patterns in the first 200 ms after stimulus onset. The pattern consists of decreased activity in posterior areas, and increased activity in parieto-frontal ones. This pattern reveals marked changes in evoked electrical activity for the elderly, although increased parieto-frontal activity did not seem to help them in the discrimination task. In addition, it seems that longer ISIs can compensate for the behavioral deficits in the elderly but do not result in comparable VEPs. The electrical source imaging results show good convergence with the fMRI literature, confirming the observation that frontal increases co-occur with posterior decreases also for electrical source activity. Since we saw no direct evidence for compensation, we tentatively interpret the pattern of activity changes as resulting from age-related neuronal decline.

REFERENCES

Aine CJ, Adair JC, Knoefel JE, Hudson D, Qualls C, Kovacevic S, Woodruff CC, Cobb W, Padilla D, Lee RR, et al. (2005): Temporal dynamics of age-related differences in auditory incidental verbal learning. Brain Res Cogn Brain Res 24:1–18.

Aine CJ, Woodruff CC, Knoefel JE, Adair JC, Hudson D, Qualls C, Bockholt J, Best E, Kovacevic S, Cobb W, et al. (2006): Aging: Compensation or maturation? Neuroimage 32:1891–904.

Arzy S, Thut G, Mohr C, Michel CM, Blanke O (2006): Neural basis of embodiment: Distinct contributions of temporoparietal junction and extrastriate body area. J Neurosci 26:8074–8081.

Bach M (1996): The Freiburg Visual Acuity test—Automatic measurement of visual acuity. Optom Vis Sci 73:49–53.

Benjamini Y, Hochberg Y (1995): Controlling the false discovery rate: A practical and powerful approach to multiple testing. J Roy Stat Soc Series B 57:289–300.

Betts LR, Taylor CP, Sekuler AB, Bennett PJ (2005): Aging reduces center-surround antagonism in visual motion processing. Neuron 45:361–366.

Birren JE, Fisher LM (1995): Aging and speed of behavior: possible consequences for psychological functioning. Annu Rev Psychol 46:329–353.

Blanke O, Mohr C, Michel CM, Pascual-Leone A, Brugger P, Seeck M, Landis T, Thut G (2005): Linking out-of-body experience and self processing to mental own-body imagery at the temporoparietal junction. J Neurosci 25:550–557.

Brodbeck V, Lascano AM, Spinelli L, Seeck M, Michel CM (2009): Accuracy of EEG source imaging of epileptic spikes in patients with large brain lesions. Clin Neurophysiol 120:679–685.

Calautti C, Serrati C, Baron JC (2001): Effects of age on brain activation during auditory-cued thumb-to-index opposition: A positron emission tomography study. Stroke 32:139–146.

Corbetta M, Kincade JM, Ollinger JM, McAvoy MP, Shulman GL (2000): Voluntary orienting is dissociated from target detection in human posterior parietal cortex. Nat Neurosci 3:292–297.

Corbetta M, Patel G, Shulman GL (2008): The reorienting system of the human brain: From environment to theory of mind. Neuron 58:306–324.

Davis SW, Dennis NA, Daselaar SM, Fleck MS, Cabeza R (2008): Que PASA? The posterior-anterior shift in aging. Cereb Cortex 18:1201–1209.

D'Esposito M, Deouell LY, Gazzaley A (2003): Alterations in the BOLD fMRI signal with ageing and disease: A challenge for neuroimaging. Nat Rev Neurosci 4:863–872.

D'Esposito M, Zarahn E, Aguirre GK, Rypma B (1999): The effect of normal aging on the coupling of neural activity to the bold hemodynamic response. Neuroimage 10:6–14.

De Santis L, Clarke S, Murray MM (2007): Automatic and intrinsic auditory "what" and "where" processing in humans revealed by electrical neuroimaging. Cereb Cortex 17:9–17.

Dickerson BC, Salat DH, Bates JF, Atiya M, Killiany RJ, Greve DN, Dale AM, Stern CE, Blacker D, Albert MS, et al. (2004): Medial temporal lobe function and structure in mild cognitive impairment. Ann Neurol 56:27–35.

Dustman RE, Shearer DE, Emmerson RY (1993): EEG and event-related potentials in normal aging. Prog Neurobiol 41:369–401.

Fahle M, Daum I (1997): Visual learning and memory as functions of age. Neuropsychologia 35:1583–1589.

Garcia-Suarez L, Barrett BT, Pacey I (2004): A comparison of the effects of ageing upon vernier and bisection acuity. Vis Res 44:1039–1045.

Gazzaley A, Clapp W, Kelley J, McEvoy K, Knight RT, D'Esposito M (2008): Age-related top-down suppression deficit in the early stages of cortical visual memory processing. Proc Natl Acad Sci USA 105:13122–13126.

Gazzaley A, Cooney JW, Rissman J, D'Esposito M (2005): Top-down suppression deficit underlies working memory impairment in normal aging. Nat Neurosci 8:1298–1300.

Genovese CR, Lazar NA, Nichols T (2002): Thresholding of statistical maps in functional neuroimaging using the false discovery rate. Neuroimage 15:870–878.

Gonzalez Andino SL, Grave de Peralta R, Khateb A, Pegna AJ, Thut G, Landis T (2007): A glimpse into your vision. Hum Brain Mapp 28:614–624.

Grady CL, Maisog JM, Horwitz B, Ungerleider LG, Mentis MJ, Salerno JA, Pietrini P, Wagner E, Haxby JV (1994): Age-related changes in cortical blood flow activation during visual processing of faces and location. J Neurosci 14(3 Part 2):1450–1462.

Grady CL, Protzner AB, Kovacevic N, Strother SC, Afshin-Pour B, Wojtowicz M, Anderson JA, Churchill N, McIntosh AR (2009): A Multivariate Analysis of Age-Related Differences in Default Mode and Task-Positive Networks across Multiple Cognitive Domains. Cereb Cortex 20(6):1432–1447.

Grave de Peralta Menendez R, Gonzalez Andino S (2002): Comparison of algorithms for the localization of focal sources: Evaluation with simulated data and analysis of experimental data. International Journal of Bioelectromagnetism 4(1). http://ijbem.k.hosei.ac.jp/2006-/volume4/number1/menendez/index.htm.

Grave de Peralta Menendez R, Gonzalez Andino S, Lantz G, Michel CM, Landis T (2001): Noninvasive localization of electromagnetic epileptic activity. I. Method descriptions and simulations. Brain Topogr 14:131–137.

Grave de Peralta Menendez R, Murray MM, Michel CM, Martuzzi R, Gonzalez Andino SL (2004): Electrical neuroimaging based on biophysical constraints. Neuroimage 21:527–539.

Groening K, Brodbeck V, Moeller F, Wolff S, van Baalen A, Michel CM, Jansen O, Boor R, Wiegand G, Stephani U, et al. (2009): Combination of EEG-fMRI and EEG source analysis improves interpretation of spike-associated activation networks in paediatric pharmacoresistant focal epilepsies. Neuroimage 46:827–833.

Gutchess AH, Welsh RC, Hedden T, Bangert A, Minear M, Liu LL, Park DC (2005): Aging and the neural correlates of successful picture encoding: Frontal activations compensate for decreased medial-temporal activity. J Cogn Neurosci 17:84–96.

Herzog MH, Koch C (2001): Seeing properties of an invisible object: Feature inheritance and shine-through. Proc Natl Acad Sci USA 98:4271–4275.

Koenig T, Prichep L, Lehmann D, Sosa PV, Braeker E, Kleinlogel H, Isenhart R, John ER (2002): Millisecond by millisecond, year by year: normative EEG microstates and developmental stages. Neuroimage 16:41–48.

Lakshminarayanan V, Enoch JM (1995): Vernier acuity and aging. Int Ophthalmol 19:109–115.

Lehmann D, Ozaki H, Pal I (1987): EEG alpha map series: Brain micro-states by space-oriented adaptive segmentation. Electroencephalogr Clin Neurophysiol 67:271–288.

Lehmann D, Skrandies W (1980): Reference-free identification of components of checkerboard-evoked multichannel potential fields. Electroencephalogr Clin Neurophysiol 48:609–621.

Levi DM, Manny RE, Klein SA, Steinman SB (1983): Electrophysiological correlates of hyperacuity in the human visual cortex. Nature 306:468–470.

Li RW, Edwards MH, Brown B (2000): Variation in vernier acuity with age. Vis Res 40:3775–3781.

Li RW, Edwards MH, Brown B (2001): Variation in vernier evoked cortical potential with age. Invest Ophthalmol Vis Sci 42:1119–1124.

Logan JM, Sanders AL, Snyder AZ, Morris JC, Buckner RL (2002): Under-recruitment and nonselective recruitment: Dissociable neural mechanisms associated with aging. Neuron 33:827–840.

Madden DJ, Whiting WL, Provenzale JM, Huettel SA (2004): Age-related changes in neural activity during visual target detection measured by fMRI. Cereb Cortex 14:143–155.

Michel CM, Murray MM, Lantz G, Gonzalez S, Spinelli L, Grave de Peralta R (2004): EEG source imaging. Clin Neurophysiol 115:2195–2222.

Michel CM, Thut G, Morand S, Khateb A, Pegna AJ, Grave de Peralta R, Gonzalez S, Seeck M, Landis T (2001): Electric source imaging of human brain functions. Brain Res Brain Res Rev 36(2–3):108–118.

Murray MM, Brunet D, Michel CM (2008): Topographic ERP analyses: A step-by-step tutorial review. Brain Topogr 20:249–264.

Murray MM, Molholm S, Michel CM, Heslenfeld DJ, Ritter W, Javitt DC, Schroeder CE, Foxe JJ (2005): Grabbing your ear: Rapid auditory-somatosensory multisensory interactions in low-level sensory cortices are not constrained by stimulus alignment. Cereb Cortex 15:963–974.

Pardo JV, Lee JT, Sheikh SA, Surerus-Johnson C, Shah H, Munch KR, Carlis JV, Lewis SM, Kuskowski MA, Dysken MW (2007): Where the brain grows old: Decline in anterior cingulate and medial prefrontal function with normal aging. Neuroimage 35:1231–1237.

Park DC, Polk TA, Park R, Minear M, Savage A, Smith MR (2004): Aging reduces neural specialization in ventral visual cortex. Proc Natl Acad Sci USA 101:13091–13095.

Park DC, Reuter-Lorenz P (2009): The adaptive brain: Aging and neurocognitive scaffolding. Annu Rev Psychol 60:173–196.

Pascual-Marqui RD, Michel CM, Lehmann D (1995): Segmentation of brain electrical activity into microstates: Model estimation and validation. IEEE Trans Biomed Eng 42:658–665.

Pekkonen E, Huotilainen M, Virtanen J, Sinkkonen J, Rinne T, Ilmoniemi RJ, Naatanen R (1995): Age-related functional differences between auditory cortices: A whole-head MEG study. Neuroreport 6:1803–1806.

Perrin F, Pernier J, Bertrand O, Giard MH, Echallier JF (1987): Mapping of scalp potentials by surface spline interpolation. Electroencephalogr Clin Neurophysiol 66:75–81.

Pfefferbaum A, Ford JM, Roth WT, Kopell BS (1980): Age-related changes in auditory event-related potentials. Electroencephalogr Clin Neurophysiol 49(3–4):266–276.

Plomp G, Mercier MR, Otto TU, Blanke O, Herzog MH (2009): Non-retinotopic feature integration decreases response-locked brain activity as revealed by electrical neuroimaging. Neuroimage 48:405–414.

Plomp G, Michel CM, Herzog MH (2010): Electrical source dynamics in three functional localizer paradigms. Neuroimage 53(1):257–267.

Poldrack RA (2000): Imaging brain plasticity: Conceptual and methodological issues—A theoretical review. Neuroimage 12:1–13.

R-Development-Core-Team (2008): R: A language and environment for statistical computing.

Resnick SM, Pham DL, Kraut MA, Zonderman AB, Davatzikos C (2003): Longitudinal magnetic resonance imaging studies of older adults: a shrinking brain. J Neurosci 23:3295–3301.

Roinishvili M, Chkonia E, Stroux A, Brand A, Herzog MH: Combining vernier acuity and visual backward masking as a sensitive test for visual temporal deficits in aging research (in revision). DOI: 10.1016/j.visres.2010.12.011.

Salat DH, Buckner RL, Snyder AZ, Greve DN, Desikan RS, Busa E, Morris JC, Dale AM, Fischl B (2004): Thinning of the cerebral cortex in aging. Cereb Cortex 14:721–730.

Salthouse TA (1996): The processing-speed theory of adult age differences in cognition. Psychol Rev 103:403–428.

Spierer L, Tardif E, Sperdin H, Murray MM, Clarke S (2007): Learning-induced plasticity in auditory spatial representations revealed by electrical neuroimaging. J Neurosci 27:5474–5483.

Spinelli L, Andino SG, Lantz G, Seeck M, Michel CM (2000): Electromagnetic inverse solutions in anatomically constrained spherical head models. Brain Topogr 13:115–125.

Srebro R, Osetinsky MV (1987): The localization of cortical activity evoked by vernier offset. Vis Res 27:1387–1390.

Vulliemoz S, Thornton R, Rodionov R, Carmichael DW, Guye M, Lhatoo S, McEvoy AW, Spinelli L, Michel CM, Duncan JS, et al. (2009): The spatio-temporal mapping of epileptic networks: Combination of EEG-fMRI and EEG source imaging. Neuroimage 46:834–843.

Waugh SJ, Levi DM, Carney T (1993): Orientation, masking, and vernier acuity for line targets. Vis Res 33:1619–1638.

Westheimer G (1975): Editorial: Visual acuity and hyperacuity. Invest Ophthalmol 14:570–572.